Evolution of the 7/2 Fractional Quantum Hall State in Two-Subband Systems

Yang Liu, J. Shabani, D. Kamburov, M. Shayegan, L. N. Pfeiffer, K. W. West, and K. W. Baldwin

Department of Electrical Engineering, Princeton University, Princeton, New Jersey 08544, USA
(Received 19 August 2011; published 20 December 2011)

We report the evolution of the fractional quantum Hall state (FQHS) at a total Landau level (LL) filling factor of $\nu = 7/2$ in wide GaAs quantum wells in which electrons occupy two electric subbands. The data reveal subtle and distinct evolutions as a function of density, magnetic field tilt angle, or symmetry of the charge distribution. At intermediate tilt angles, for example, we observe a strengthening of the $\nu = 7/2$ FQHS. Moreover, in a well with asymmetric change distribution, there is a developing FQHS when the LL filling factor of the symmetric subband ν_S equals 5/2 while the antisymmetric subband has a filling factor of $1 < \nu_A < 2$.

The fractional quantum Hall states (FQHSs) at even-denominator Landau level (LL) filling factors [1] have recently come into the limelight thanks to the theoretical prediction that these states might be non-Abelian [2] and be useful for topological quantum computing [3]. This expectation has spawned a flurry of investigations, both experimental [4–10] and theoretical [11–13], into the origin and stability of the even-denominator states. Much of the attention has been focused on the $\nu = 5/2$ FQHS which is observed in very low disorder two-dimensional electron systems (2DESs) when the Fermi energy (E_F) lies in the spin-up, excited-state $(N = 1)$, LL of the ground state (symmetric, S) electric subband, namely, in the $S1\uparrow$ level. Here we examine the stability of the FQHS at $\nu = 7/2$, another even-denominator FQHS, typically observed when E_F is in the $S1\downarrow$ level [Fig. 1(a)] [4,7]. The $\nu = 7/2$ FQHS, being related to the 5/2 state through particle-hole symmetry, is also theoretically expected to be non-Abelian. Our study, motivated by theoretical proposals that the even-denominator FQHSs might be favored in 2DESs with "thick" wave functions [11–13], is focused on electrons confined to wide GaAs quantum wells (QWs). In a realistic, experimentally achievable wide QW, however, the electrons at $\nu = 7/2$ can occupy the second (antisymmetric, A) electric subband when the subband energy spacing (Δ) is comparable to the cyclotron energy $\hbar\omega_c$ [Figs. 1(b)–1(d)]. Here we experimentally probe the stability of the $\nu = 7/2$ FQHS in wide QW samples with tunable density in the vicinity of the crossings (at E_F) between the $S1$ and the $A0$ LLs.

Our samples were grown by molecular beam epitaxy, and each consists of a wide GaAs QW bounded on each side by undoped $Al_{0.24}Ga_{0.76}As$ spacer layers and Si δ-doped layers. We report here data, taken at $T \simeq$ 30 mK, for three samples with QW widths of $W = 37$, 42, and 55 nm. The QW width and electron density (n) of each sample were designed so that its Δ is close to $\hbar\omega_c$ at the magnetic field position of $\nu = 7/2$. This enables us to make the $S1$ and the $A0$ LLs cross at E_F by tuning n or the

charge distribution asymmetry, which we achieve by applying back- and front-gate biases [7,14–16]. For each n, we measure the occupied subband electron densities n_S and n_A from the Fourier transforms of the low-field ($B \leq$ 0.5 T) Shubnikov–de Haas oscillations [14,15], and determine $\Delta = (\pi\hbar^2/m^*)(n_S - n_A)$, where $m^* = 0.067m_e$ is the GaAs electron effective mass. At a fixed total density, Δ is smallest when the charge distribution is "balanced" (symmetric) and it increases as the QW is imbalanced. Our measured Δ agree well with the results of calculations that solve the Poisson and Schrödinger equations to obtain the potential energy and the charge distribution self-consistently [see, e.g., Figs. 1(a) and 1(d)].

Figure 1 shows a series of longitudinal (R_{xx}) and Hall (R_{xy}) resistance traces in the range $3 < \nu < 4$ for a 42-nm-wide QW sample, taken at different n from 2.13 to 2.96 × 10^{11} cm^{-2} while keeping the total charge distribution balanced. As n is increased in this range, Δ decreases from 64 to 54 K while $\hbar\omega_c$ at $\nu = 7/2$ increases from 50 to 70 K, so we expect crossings between the $S1$ and $A0$ levels, as illustrated in Figs. 1(a)–1(d). These crossings manifest themselves in a remarkable evolution of the FQHSs as seen in Fig. 1. At the lowest n, which corresponds to the LL diagram shown in Fig. 1(a), R_{xx} shows a reasonably deep minimum at $\nu = 7/2$, accompanied by a clear inflection point in R_{xy} at $7/2(h/e^2)$, and a weak minimum near $\nu = 10/3$. These features are characteristic of the FQHSs observed in high-quality, standard (single-subband) GaAs 2DESs, when E_F lies in the $S1\downarrow$ LL [4,7]. As n is raised, we observe an R_{xx} spike near $\nu = 7/2$, signaling a crossing of $S1\downarrow$ and $A0\uparrow$. At $n = 2.51 ×$ 10^{11} cm^{-2}, these levels have crossed, and E_F is now in $A0\uparrow$ [Fig. 1(b)]. There is no longer a minimum at $\nu = 7/2$ and instead, there are very strong minima at $\nu = 10/3$ and 11/3. Further increasing n causes a crossing of $S1\uparrow$ and $A0\uparrow$ and, at $n = 2.63 × 10^{11}$ cm^{-2}, E_F at $\nu = 7/2$ lies in $S1\uparrow$ [Fig. 1(c)]. Here the R_{xx} minimum and R_{xy} inflection point at $\nu = 7/2$ reappear, signaling the return of a FQHS. As we increase n even further, $S1\uparrow$ and $A0\downarrow$ cross and, at
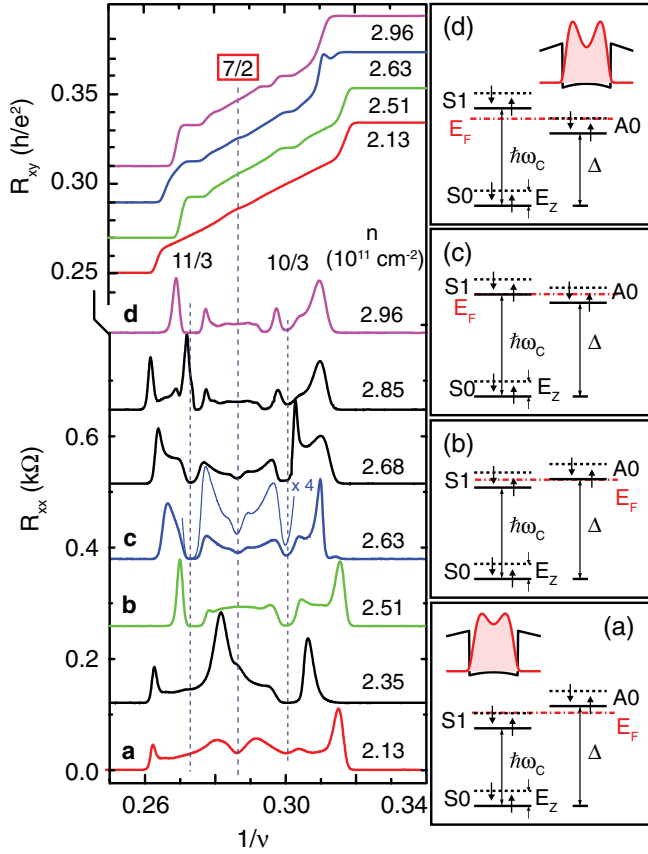
FIG. 1 (color online).   Left panel: Waterfall plot of R_{xx} and R_{xy} traces at different densities for a 42-nm-wide GaAs QW. (a)–(d) Schematic LL diagrams at $\nu = 7/2$ for different densities corresponding to the traces marked **a**–**d** in the left panel. The subband separation, cyclotron, and Zeeman energies are marked as Δ, $\hbar\omega_c$, and E_Z, respectively. Self-consistently calculated charge distributions are shown in the insets to (a) and (d) for $n = 2.13$ and 2.96×10^{11} cm^{-2}.

$n = 2.96 \times 10^{11}$ cm^{-2}, when E_F at $\nu = 7/2$ lies in $A0\!\downarrow$, there is again no $\nu = 7/2$ minimum but there are strong FQHSs at $\nu = 10/3$ and $11/3$.

The above observations provide clear and direct evidence that the even-denominator $\nu = 7/2$ FQHS is stable when E_F is in an excited ($N = 1$) LL but not when E_F lies in a ground state ($N = 0$) LL [7]. Examining traces taken at numerous other n, not shown in Fig. 1 for lack of space, reveal that the appearances and disappearances of the $\nu = 7/2$ FQHS are sharp, similar to the behavior of the $5/2$ FQHS at a LL crossing [17]. It is noteworthy that when the two crossing levels have *antiparallel* spins, a "spike" in R_{xx} at the crossing completely destroys the FQHS at $\nu = 7/2$ and nearby fillings. At the crossing of two levels with *parallel* spins, on the other hand, there is no R_{xx} spike. These behaviors are reminiscent of easy-axis and easy-plane ferromagnetism for the antiparallel- and parallel-spin crossings, respectively [16,18].

Next, we examine the evolution of the $\nu = 7/2$ FQHS in the presence of a parallel magnetic field component $B_\parallel$,
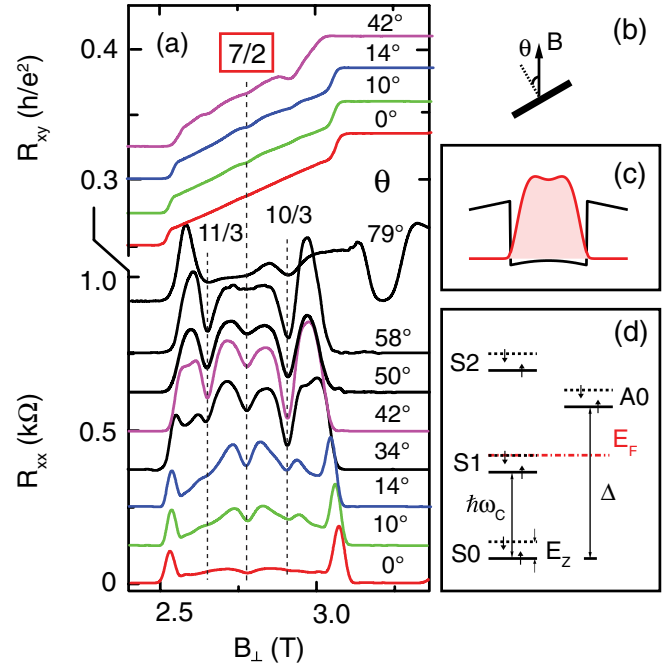

FIG. 2 (color online).   (a) R_{xx} and R_{xy} traces for a 37-nm-wide GaAs QW at $n = 2.34 \times 10^{11}$ cm^{-2} at different tilt angles θ as depicted in (b). (c) Charge distribution calculated self-consistently at $B = 0$. (d) LL diagram at $\theta = 0$ at $\nu = 7/2$.

introduced by tilting the sample so that its normal makes an angle θ with the total field direction [Fig. 2(b)]. Figure 2(a) captures this evolution for electrons confined to a symmetric, 37-nm-wide QW [19]. This QW is narrower so that, at $n = 2.34 \times 10^{11}$ cm^{-2}, its Δ ($= 82$ K) is well above $\hbar\omega_c$ ($= 55$ K). The $\theta = 0$ trace then corresponds to E_F lying in $S1\!\downarrow$, as shown in Fig. 2(d). As θ is increased, we observe only a gradual change in the strength of the $\nu = 7/2$ FQHS, until it disappears at large $\theta \gtrsim 55°$. This is not surprising since, in a two-subband system like ours, we expect a severe mixing of the LLs of the two subbands with increasing θ [20] rather than sharp LL crossings as manifested in Fig. 1 data.

We highlight three noteworthy features of Fig. 2 data. First, the $\nu = 7/2$ R_{xx} minimum persists up to relatively large θ (up to 50°), and it even appears that the R_{xy} plateau is better developed at finite θ (up to $\theta = 42°$) compared to $\theta = 0$, suggesting a strengthening of the $7/2$ FQHS at intermediate angles. Second, deep R_{xx} minima develop with increasing θ at $\nu = 10/3$ and $11/3$, implying the development of reasonably strong FQHSs at these fillings. This is consistent with the results of Xia *et al.* who report a similar strengthening of the $7/3$ and $8/3$ states—the equivalent FQHSs flanking the $\nu = 5/2$ state in the $S1\!\uparrow$ level—when a wide QW sample is tilted in field [9]. It is particularly remarkable that, at intermediate θ ($\simeq 40°$), there are well-developed FQHSs at $\nu = 10/3$ and $11/3$ *as well as* at $\nu = 7/2$. Third, the large magnitude of $B_\parallel$ at the highest angles appears to greatly suppress Δ, rendering

the electron system essentially into a bilayer system [21]. This is evidenced by the dramatic decrease in the strength of the $\nu = 3$ QHS and the disappearance of the $\nu = 11/3$ R_{xx} minimum at $\theta = 79°$; note that a FQHS should not exist at $\nu = 11/3$ in a bilayer system with two isolated 2DESs as such a state would correspond to 11/6 filling in each layer.

We now focus on data taken on a 55-nm-wide QW where we keep the total n fixed and change the charge distribution symmetry by applying back- and front-gate biases with opposite polarity. In Fig. 3(a) we show a set of R_{xx} traces, each taken at a different amount of asymmetry. The measured Δ is indicated for each trace and ranges from 14 K for the symmetric charge distribution to 70 K for a highly asymmetric distribution. In Fig. 3(b) we present a color-scale plot of R_{xx} with B and Δ as x and y axes, based on an interpolation of Fig. 3(a) data and many other traces taken at different values of Δ. When the charge distribution is symmetric or nearly symmetric in this QW, $\Delta \simeq 14$ K is much smaller than $\hbar\omega_c$ (= 85 K at $\nu = 7/2$) so that the LL diagram is qualitatively the one shown in Fig. 1(d). Consistent with this LL diagram, we observe a very strong $\nu = 4$ QHS. Also, since E_F lies in the $A0\!\!\downarrow$ level at $\nu = 7/2$, there is no $\nu = 7/2$ FQHS and instead we observe strong FQHSs at $\nu = 10/3$ and $11/3$. As Δ is increased, we expect

a crossing of $S1\!\!\uparrow$ and $A0\!\!\downarrow$, leading to a destruction of the $\nu = 4$ QHS at the crossing. This is indeed seen in Figs. 3(a) and 3(b). What is striking, however, is that the $\nu = 4$ R_{xx} minimum disappears over a very large range of Δ, between 35 and 62 K. Even more remarkable are several anomalous R_{xx} minima in this range of Δ in the filling range $3 < \nu < 5$, particularly those marked by arrows in Fig. 3(a). These minima resemble what is observed in the top trace but are seen at lower fields.

These features betray a pinning together, at E_F, of the partially occupied $S1\!\!\uparrow$ and $A0\!\!\downarrow$ levels, and a charge transfer between them, in a finite range of B and gate bias. As pointed out in Ref. [22], when only a small number of quantized LLs belonging to two different subbands are occupied, the distribution of electrons between these levels does not necessarily match the $B = 0$ subband densities. This leads to a mismatch between the total electron charge density distributions at $B = 0$ and high B, which is given by

$$\rho(B) = e(eB/h)[\nu_S|\psi_S(B)|^2 + \nu_A|\psi_A(B)|^2], \quad (1)$$

where ν_S and ν_A are the fillings of the S and A subbands and $\psi_S(B)$ and $\psi_A(B)$ are the in-field subband wave functions. The pinning and the inter-LL charge transfer help bring these distributions closer to each other [22,23].
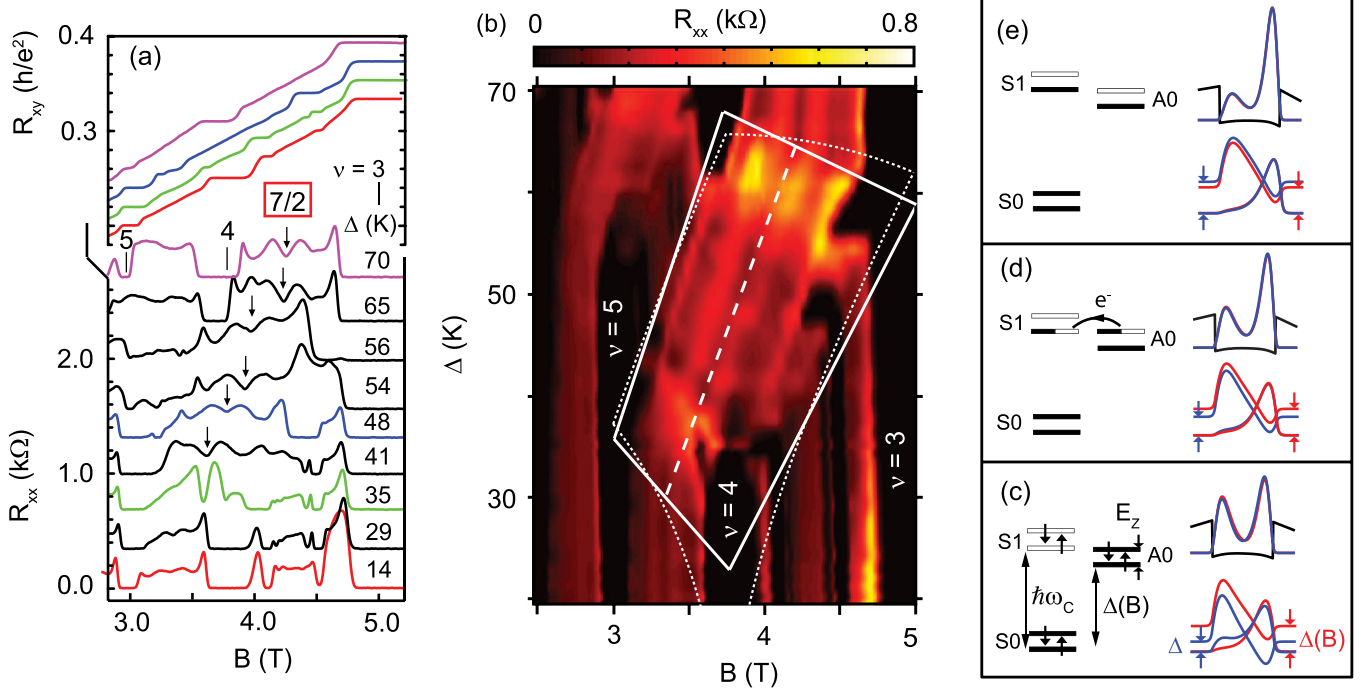

FIG. 3 (color online). (a) R_{xx} and R_{xy} traces for a 55-nm-wide GaAs QW, at a fixed $n = 3.62 \times 10^{11}$ cm^{-2}, as the charge distribution is made increasingly asymmetric. Values of Δ, measured from low-B Shubnikov–de Haas oscillations, are indicated for each trace. Vertical arrows mark the positions of observed anomalous R_{xx} minima. (b) A color-scale plot of data in (a). Solid and dotted lines are the calculated boundary within which the $S1\!\!\uparrow$ and $A0\!\!\uparrow$ levels are pinned together at E_F [24]. The dashed line represents the values of B at which, according to the calculations, the $S1\!\!\uparrow$ level is half-filled; it tracks the positions of the observed R_{xx} minima marked by vertical arrows in (a). (c)–(e) Schematic LL diagrams (left), charge distributions and potentials (upper right), and wave functions ψ_S and ψ_A (lower right), self-consistently calculated at $B = 0$ (blue) and at $\nu = 4$ (red). In (c)–(e), the filling factor of the $S1\!\!\uparrow$ level equals 0, 0.5, and 1, respectively. In each panel, the calculated wave functions are shifted vertically according to the calculated values of Δ and $\Delta(B)$.

P H Y S I C A L   R E V I E W   L E T T E R S

To demonstrate such a pinning quantitatively and determine the boundary inside which the $S1\uparrow$ and $A0\downarrow$ levels are pinned together, we performed self-consistent calculations of the potential energy and charge distribution at high B for different QW asymmetries [24]. The calculated boundary is shown by solid white lines in Fig. 3(b), and examples of the results of our calculations (at $\nu = 4$) are shown in Figs. 3(c)–3(e). When we imbalance the QW at $\nu = 4$, at the lower boundary, as the $A0\downarrow$ level reaches the $S1\uparrow$ level from below, $\nu_S = \nu_A = 2$ [Fig. 3(c)]. As we further imbalance the QW, electrons are transferred from $A0\downarrow$ to the $S1\uparrow$ level, while these two levels are pinned together and $\Delta(B) = \hbar\omega_c - E_Z$ remains unchanged. The charge transfer ends at the upper boundary when $\nu_S = 3$ and $\nu_A = 1$ [Fig. 3(e)]. In our calculations, we use ($\nu_S = \nu_A = 2$) or ($\nu_S = 3$, $\nu_A = 1$) in Eq. (1) and find the zero-field subband spacings Δ for the two particular QW asymmetries which give an in-field subband spacing equal to $\Delta(B) = \hbar\omega_c - E_Z$ [24]. The boundary at other magnetic fields in the range $3 \leq \nu \leq 5$ is calculated in a similar fashion [24]. In Fig. 3(b), it is clear that the calculated boundary matches reasonably well the region (in Δ vs B plane) in which we experimentally observe a disappearance of the $\nu = 4$ R_{xx} minimum and the appearance of R_{xx} minima at anomalous fillings. This matching is particularly remarkable considering that there are no adjustable parameters in our simulations, except for using a single value (7.3) for the enhanced g factor [24].

In Fig. 3(b) we include a dashed line representing the values of B at which, according to our calculations, the $S1\uparrow$ level is exactly half-filled, i.e., $\nu_S = 5/2$ and $\nu_A = (\nu - 5/2)$. This dashed line tracks the positions of the observed R_{xx} minima marked by the vertical arrows in (a) very well, suggesting that these minima indeed correspond to $\nu_S = 5/2$ [25]. This is an astonishing observation, as it implies a developing FQHS at 5/2 filling of the symmetric subband even when a partially filled $A0\downarrow$ level is pinned to the half-filled $S1\uparrow$ level at E_F.

We remark that while LL pinning in two-subband systems is a general phenomenon [22], its manifestation is more pronounced in bilayerlike electron systems with asymmetric (imbalanced) charge distributions [23]. For example, we do not see signatures of LL pinning in the data of Fig. 1 which were taken on an electron system with a symmetric (balanced) charge distribution. This is because an intersubband charge transfer barely changes the total charge distribution in this balanced QW. In wide ($W = 60$ and 80 nm) GaAs QWs with imbalanced charge distributions, on the other hand, in an independent study Nuebler *et al.* [26] observed a pining of the $S1\uparrow$ and $A0\uparrow$ levels, leading to the formation of a FQHS when $\nu_S = 5/2$ while the $A0\uparrow$ level is partially occupied.

In summary, our results reveal distinct metamorphoses of the ground state of two-suband 2DESs at and near $\nu = 7/2$ as either the magnetic field is tilted, or the density or the

charge distribution symmetry are varied. Most remarkably, we observe an apparent strengthening of the $\nu = 7/2$ FQHS at intermediate tilt angles, and a developing FQHS when a half-filled $S1\uparrow$ level is pinned to a partially filled $A0\downarrow$ level.

[1] R. L. Willett, J. P. Eisenstein, H. L. Störmer, D. C. Tsui, A. C. Gossard, and J. H. English, Phys. Rev. Lett. **59**, 1776 (1987).

[2] G. Moore and N. Read, Nucl. Phys. **B360**, 362 (1991).

[3] C. Nayak, S. H. Simon, A. Stern, M. Freedman, and S. Das Sarma, Rev. Mod. Phys. **80**, 1083 (2008).

[4] C. R. Dean, B. A. Piot, P. Hayden, S. Das Sarma, G. Gervais, L. N. Pfeiffer, and K. W. West, Phys. Rev. Lett. **100**, 146803 (2008).

[5] H. C. Choi, W. Kang, S. Das Sarma, L. N. Pfeiffer, and K. W. West, Phys. Rev. B **77**, 081301 (2008).

[6] J. Nuebler, V. Umansky, R. Morf, M. Heiblum, K. von Klitzing, and J. Smet, Phys. Rev. B **81**, 035316 (2010).

[7] J. Shabani, Y. Liu, and M. Shayegan, Phys. Rev. Lett. **105**, 246805 (2010).

[8] A. Kumar, G. A. Csáthy, M. J. Manfra, L. N. Pfeiffer, and K. W. West, Phys. Rev. Lett. **105**, 246808 (2010).

[9] J. Xia, V. Cvicek, J. P. Eisenstein, L. N. Pfeiffer, and K. W. West, Phys. Rev. Lett. **105**, 176807 (2010).

[10] W. Pan, N. Masuhara, N. S. Sullivan, K. W. Baldwin, K. W. West, L. N. Pfeiffer, and D. C. Tsui, Phys. Rev. Lett. **106**, 206806 (2011).

[11] E. H. Rezayi and F. D. M. Haldane, Phys. Rev. Lett. **84**, 4685 (2000).

[12] M. R. Peterson, T. Jolicoeur, and S. Das Sarma, Phys. Rev. Lett. **101**, 016807 (2008); Phys. Rev. B **78**, 155308 (2008).

[13] A. Wójs, C. Tőke, and J. K. Jain, Phys. Rev. Lett. **105**, 096802 (2010).

[14] Y. W. Suen, H. C. Manoharan, X. Ying, M. B. Santos, and M. Shayegan, Phys. Rev. Lett. **72**, 3405 (1994).

[15] J. Shabani, T. Gokmen, Y. T. Chiu, and M. Shayegan, Phys. Rev. Lett. **103**, 256802 (2009).

[16] Yang Liu, J. Shabani, and M. Shayegan, Phys. Rev. B **84**, 195303 (2011).

[17] Y. Liu, D. Kamburov, M. Shayegan, L. Pfeiffer, K. West, and K. Baldwin, Phys. Rev. Lett. **107**, 176805 (2011).

[18] K. Muraki, T. Saku, and Y. Hirayama, Phys. Rev. Lett. **87**, 196801 (2001).

[19] Application of a $B_\parallel$ component leads to an anisotropic state at intermediate tilt angles. Traces shown in Fig. 2 were taken along the hard axis; data along the easy axis show a qualitatively similar behavior.

[20] N. Kumada, K. Iwata, K. Tagashira, Y. Shimoda, K. Muraki, Y. Hirayama, and A. Sawada, Phys. Rev. B **77,** 155324 (2008).

[21] J. Hu and A. H. MacDonald, Phys. Rev. B **46,** 12 554 (1992). According to this work, in a bilayer system with interlayer distance d, $\Delta \sim \exp[-(\frac{d}{2l_B}\tan(\theta))^2]$ where l_B is the magnetic length. For a crude estimate of Δ in parallel field in our sample, if we use the distance between the peaks in the charge distribution [Fig. 2(c)] as d, we find that $\Delta \simeq \hbar\omega_c$ near $\sim 55°$, and $\Delta \lesssim 1$ K at $\theta = 80°$.

[22] S. Trott, G. Paasch, G. Gobsch, and M. Trott, Phys. Rev. B **39,** 10 232 (1989).

[23] A. G. Davies, C. H. W. Barnes, K. R. Zolleis, J. T. Nicholls, M. Y. Simmons, and D. A. Ritchie, Phys. Rev. B **54,** R17 331 (1996); V. T. Dolgopolov, A. A. Shashkin, E. V. Deviatov, F. Hastreiter, M. Hartung, A. Wixforth, K. L.

Campman, and A. C. Gossard, *ibid.* **59,** 13 235 (1999); V. V. Solovyev, S. Schmult, W. Dietsche, and I. V. Kukushkin, *ibid.* **80,** 241310 (2009).

[24] See Supplemental Material at http://link.aps.org/supplemental/10.1103/PhysRevLett.107.266802 for a detailed description of our self-consistent calculations, as well as a simple analytic model whose results are shown by dotted lines in Fig. 3(b).

[25] On each side of the dashed line in Fig. 3(b), there is a dark region running parallel to it. These regions represent the broad R_{xx} minima we observe on the flanks of the R_{xx} minima marked by arrows in Fig. 3(a). These broad minima correspond to $\nu_S \simeq 7/3$ or $8/3$.

[26] J. Nuebler, B. Friess, V. Umansky, B. Rosenow, M. Heiblum, K. v. Klitzing, and J. Smet, arXiv:1109.6219 [Phys. Rev. Lett. (to be published)].